Green Synthesis of Heteroatom Doped Graphene from Natural and Chemical Precursors for Oxygen Reduction Reaction

Sedigheh Sadegh Hassani [a], Leila Samiee [b*]

[a] Catalysis Research Division, Research Institute of Petroleum Industry (RIPI), Tehran, Tehran, Iran.
[b] Energy Technology Research Division, Research Institute of Petroleum Industry (RIPI), Tehran, Tehran, Iran.

ABSTRACT

In the present work, natural biomass and chemical materials were applied as the heteroatom resources for modifying the Porous Graphene (PG) structure by pyrolysis method at 900 ºC. The physical and chemical characterizatons were performed by means of Scanning Electron Microscopy (SEM), Brunauer–Emmett–Teller (BET), Raman Spectroscopy, N_2 Adsorption-Desorption, and X-ray Photo-electron Spectroscopy (XPS). Furthemore, the behavior of the prepared materials was investigated by Cyclic Voltammetry (CV) and Rotating Disk Electrode (RDE). The obtained results indicated that doping of heteroatoms into the graphene framework was possible using a low-cost and environment-friendly biomass material as well as chemical sources. Moreover, one-step quarternary and tersiary co-doped graphene could be acheived using natural biomass. The prepared electrocatalysts using grape leaves and sulfur trioxide pyridine complex exhibit higher electrocatalytic performance as exampled which conducted the electrocatalyst in 4e⁻ pathway and showed high stability in methanol solutions during the process, confirming their considerable potential to Oxygen Reduction Reaction (ORR) as an electro-catalyst. Moreover, the onset potential of Gl300G-900 and GSP 900 (0.93 V vs RHE) is almost equal to the Pt/C 20 wt % (0.99 V vs RHE). These optimal prepared cathodes (Gl300G-900 and GSP 900) in the Microbial Fuel Cell (MFC) test lead to considerable power densities of 31.5 mW m⁻² and 30.9.mW m⁻², which are close to 38.6 mW m⁻² for the Pt/C 20 wt % cathode.

1. INTRODUCTION

The demand for sustainable and clean energy technologies has been arising due to the growing energy consumption and environmental pollutions. Fuel cells, supercapasitors, and Li ion batteries as clean energy devices are able to transform the chemical energy to electricity [1, 2].

However, because of such problems as slow electron transfer kinetics for oxygen reduction reaction, this reaction is subject to limitations that cause performance losses [3, 4]. Therefore, development of highly efficient cathodic ORR catalysts is so necessary. Platinum and its derivities are the most active electrocatalysts for the ORR; however, their cost, limited Pt resources, susceptibility to methanol crossover, low durability, and slow electron transfer kinetics for ORR are the challenges that should be considered before large-scale use. Thus, a probe into finding new high-performance non-precious electrocatalyst for ORR has drawn greater interest [5-7].

Recently, for increasing electrical conductivity and activity, heteroatom-doped carbon materials were applied in electrocatalysis ORR, supercapacitors, and metal-air batteries. Doping the heteroatoms such as sulfur, nitrogen, phosphorus, and boron into the graphene nanosheets enhances electrical properties of the grapheneas and effectively creates more active sites in the elecatalyst towards the ORR [8, 9].

Due to the difference between the electronegativity of heteroatoms (N: 3.04, S: 2.58, I: 2.66, B: 2.04) and the carbon base (2.55), the electroneutrality of the adjacent carbon will change [10, 11]. Furthemore, the electronic density of states near the Fermi level will increse. Boron and phosphorus with lower electronegativity than carbon create a partial negative charge on the carbon atom. However, a partial positive charge will be obtained on the adjacent carbon atom. Moreover, upon introducing the heteroatoms in the carbon lattice, the C–C bond length may change, thus making the carbon surfaces asymmetrical and providing more defects as the active sites facilitate the O_2 adsorption during the ORR process [11-13].

Different approaches and many chemicals with high cost and hazardous properties have been used for introducing hetero-atoms within the graphene framework [14, 15]. In situ doping and post-synthesis methods are the two main techniques for doping heteroatoms in the carbon structres. Chemical vapor deposition, arc discharge, solvothermal approach, laser ablation, microwave irradiation, and segregation growth approach are used for insitu method. Thermal treatment of previously prepared carbon in the presence of a heteroatom source and wet chemical approach are the most important techniques for post-synthesis doping. The details of the advantages and disadvantages of each method have been discussed in the literature. However, the

post-synthesis doping technique will only lead to surface doping of the structure, while the in situ technique could lead to more homogeneous doping of the carbon material [16].

Moreover, due to economic and safety purpose, a few papers have been focused on green synthesis of ORR electrocatalysts using biomass resources such as mushroom and microalgae *Synechococcus elangatus* for investigating the possibility of introducing heteroatoms to carbon framework [17-19]. Therefore, this paper is focused on some available natural resources including garlic and Grape Leaves (Gl) as new and economic materials for ORR. The electrochemical performances were compared with our last works [19, 20], in which the microalgae Synechococcus elangatus and Sulfur Trioxide Pyridine (STP) complex were applied as the dopants. The studied electrode had superior stability to the conventional 20 wt %/C eletrocatalyst under alkaline conditions.

2. EXPERIMENTAL

2.1. Materials and reagents

The Garlic and grape leaves were obtained from Tehran garden in Iran. The Synechococcus elangatus cyanobacterium was prepared according to our last paper [19]. Sulfur trioxide pyridine complex, Nafion solution (5 wt % in alcohols-water), KOH, HCl (37 %), and Ethanol (99.8 %) were purchased from Sigma-Aldrich Company. Also, Pt/C 20 wt % was also obtained from Sigma-Aldrich Company.

2.2. Synthesis of samples

Porous graphene was synthesized by CVD method and its purification was made possible and used as a conductive support according to the litrature [20, 21]. The doped-graphene was synthasized using micro-algae according to the reported procedure [19]. Homogeneous carbonized microalgae at 300 °C at a ratio of 2:1 was ball milled with porous graphene at 300 rpm for 1 h and pyrolyzed under inert atmosphere at 900 °C for 2 h. The synthesized sample is J300G-900. The garlic and fresh grape leaves as the heteroatom sources were dried at 60 °C in a vacuum drying oven. The dried powders were ground into fine powder and carbonized at 300 °C, separately.

Homogeneous carbonized powders of these two natural sorces at a mass ratio of 2:1 were mixed with graphene and ground by ball-mill at 300 rpm for 1 h. The produced mixtures (Grape leaves@graphene and garlic@graphene) were subsequently pyrolyzed under N_2 atmosphere in a furnace at 900 °C for 2 h to synthesize a heteroatom-doped graphene Gl300G-900 and S300G-900, respectively. The PG and sulfur trioxide pyridine complex were mixed and dried according to our last work [20]. The dried powder was ground and pyrolyzed in the N_2 atmosphere at 900 °C for 2 h. The catalysts synthesized in this condition will be here referred with GSP 900. The overall synthesis process is shown in Figure 1.

3. METHOD

3.1. Methodology

3.1.1. Characterizations techniques

A Kemiat DX-27 device using CuK_α radiation was applied to obtain the XRD pattern between 10-80°. FESEM Mira-

TSCAN equipped EDS mapping was used for morphology analysis. The nitrogen adsorption/desorption experiment was applied using a micromeritics Tristar 3000 instrument. The Raman spectroscopy Almega Thermo Nicolet with an Ar ion laser source (514 nm) was used. Furthermore, XPS Model 5700 by Al Kα (1486.6 eV photons) was utilized for surface chemical composition determination. Multipak™ software package was used for data processing and a Shirley background subtraction routine was applied throughout.
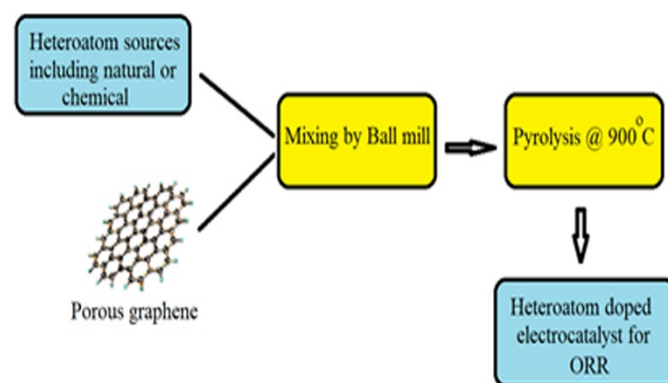

Figure 1. Schematic of heteroatom-doped graphene synthesis

3.1.2. Electrochemical measurements

A three-electrode Autolab potentiostat/galvanostat was applied to electrochemical evaluation. The Ag/AgCl and platinum wire were utilized as the reference and counter electrodes, respectively.

A 5 mg mL^{-1} suspension was prepared using sonicating of electrocatalyst in a ethanol-nafion solution for 30 minutes and pipetted onto glassy carbon electrode as a working electrode and dried in air at 60 °C to obtain 0.3 mg cm^{-2} electrocatalyst loading on the glassy carbon electrode.

Linear sweep voltammetry using a rotating disk electrode was applied in the O_2-saturated 0.1 M KOH solution (pH=13) in the potential ranges from -1 to 0.2 V at a scan rate of 5 mV s^{-1} and different rpms. Electron transfer was calculated using the Koutecky–Levich equation. Moreover, cyclic voltammetry tests were measured at a scan rate of 50 mV/s within a voltage range of 0.2 V to -1.0 V (vs. Ag/AgCl electrode).

4. RESULTS AND DISCUSSION

4.1. Electrochemical evaluation

4.1.1. Cyclic voltammetric results

The electrocatalytic evaluation of the synthesized electrocatalyst including chemical and natural pecursors (Gl300G-900, S300G-900 and J300G-900 and GSP 900) was conducted using CV in the O_2 saturated 0.1 M KOH solution and the results were compared with Pt/C 20 wt % and PG samples (Figure 2).

The onset potential of PG in the ORR (after about 20 CV cycles) was about 0.82 V (versus RHE), where the oxygen reduction peak appreared approximately at 0.73 V (versus RHE). All the prepared samples showed ORR reduction peak with greater intensity, improved onset potential, and increased peak current density than porous graphene. These obtained results showed that catalyst performance could be boosted by doping heteroatom into the graphene structure.
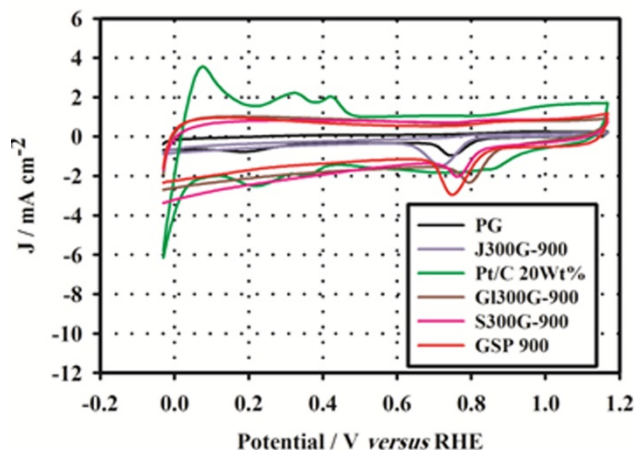
Figure 2. CV of samples for ORR in O_2 saturated 0.1 M KOH at a sweep rate of 50 mV/s on the: S300G-900, J300G-900, Gl300G-900, GSP 900 PG and Pt/C 20 wt %, electrodes

4.1.2. Rotating disk electrode test

The electrocatalytic performance of the synthesized samples was studied using an RDE in the range rotation speeds of 250 to 3500 rpm. Furthermore, the Koutechy–Levich equation was used to determine the number of electron transfer involved in the ORR. These equations are illustrated in the following [22, 23]:

$$\frac{1}{j} = \frac{1}{j_k} + \frac{1}{j_d} = \frac{1}{j_k} + \frac{1}{B\omega^{1/2}} \tag{1}$$

$$j_d = 0.62\, n \times F \times (C_0) \times (D_0)^{\frac{2}{3}} \times (A)^{\frac{-1}{6}} = B\omega^{\frac{1}{2}} \tag{2}$$

$$B = 0.62\, n \times F \times (C_0) \times (D_0)^{\frac{2}{3}} \times (A)^{\frac{-1}{6}} \tag{3}$$

The measured current density, diffusion, and kinetic limiting current densities are shown with J, J_L and J_K, respectively. F is the Faraday constant (96485 C/mol); n and ω are the electron transfer number and the rotation speed (rpm), respectively. Furthermore, the bulk concentration of O_2 (C_0), the diffusion coefficient of oxygen (D_0) in 0.1 M KOH as electrolyte, and kinetic viscosity (v) are 1.2×10^{-6} mol/cm^3, 1.9×10^{-5} cm^2/s, and 0.01 cm^2/s, respectively.

The J^{-1} versus $\omega^{-0.5}$ plots in the potential range of 0.45 to 0.65 (V vs RHE) are shown in Figure 3 and Table 1, suggesting both 2e$^-$ and 4e$^-$ for ORR in different electrocatalysts. The heteroatom-doped graphenes Gl300G-900 and GSP 900 as the synthesized samples using grape leaves and sulfur trioxide pyridine complex show reasonable selectivity to the 4 electron reaction pathway and improved onset potential in an alkaline electrolyte, respectively.

LSV curves for electrocatalysts in the O_2 saturated 0.1 M KOH electrolyte at a scan rate of 5 mv/s and a rotation rate of 1500 compared to Pt/C 20 wt % and PG are shown in Figure 4.
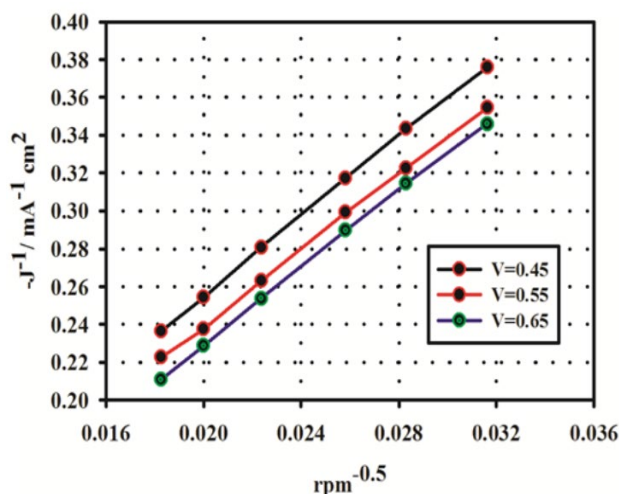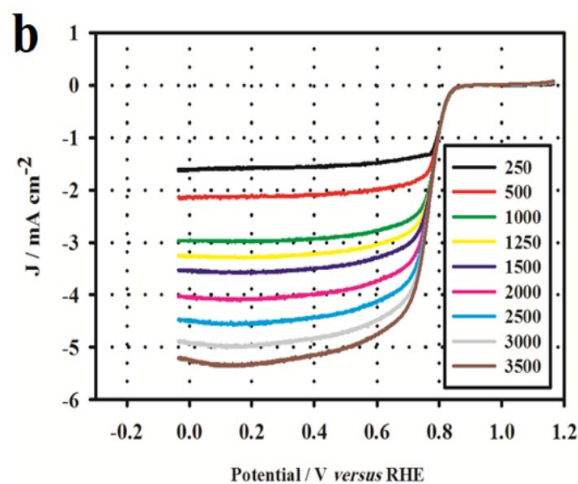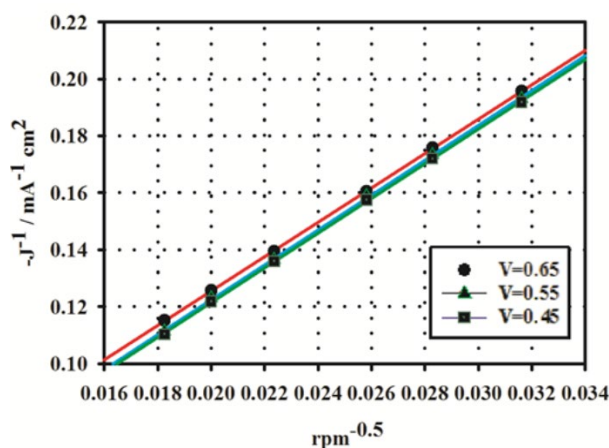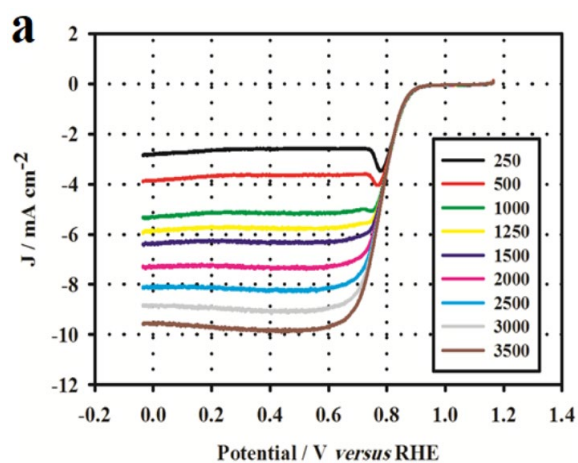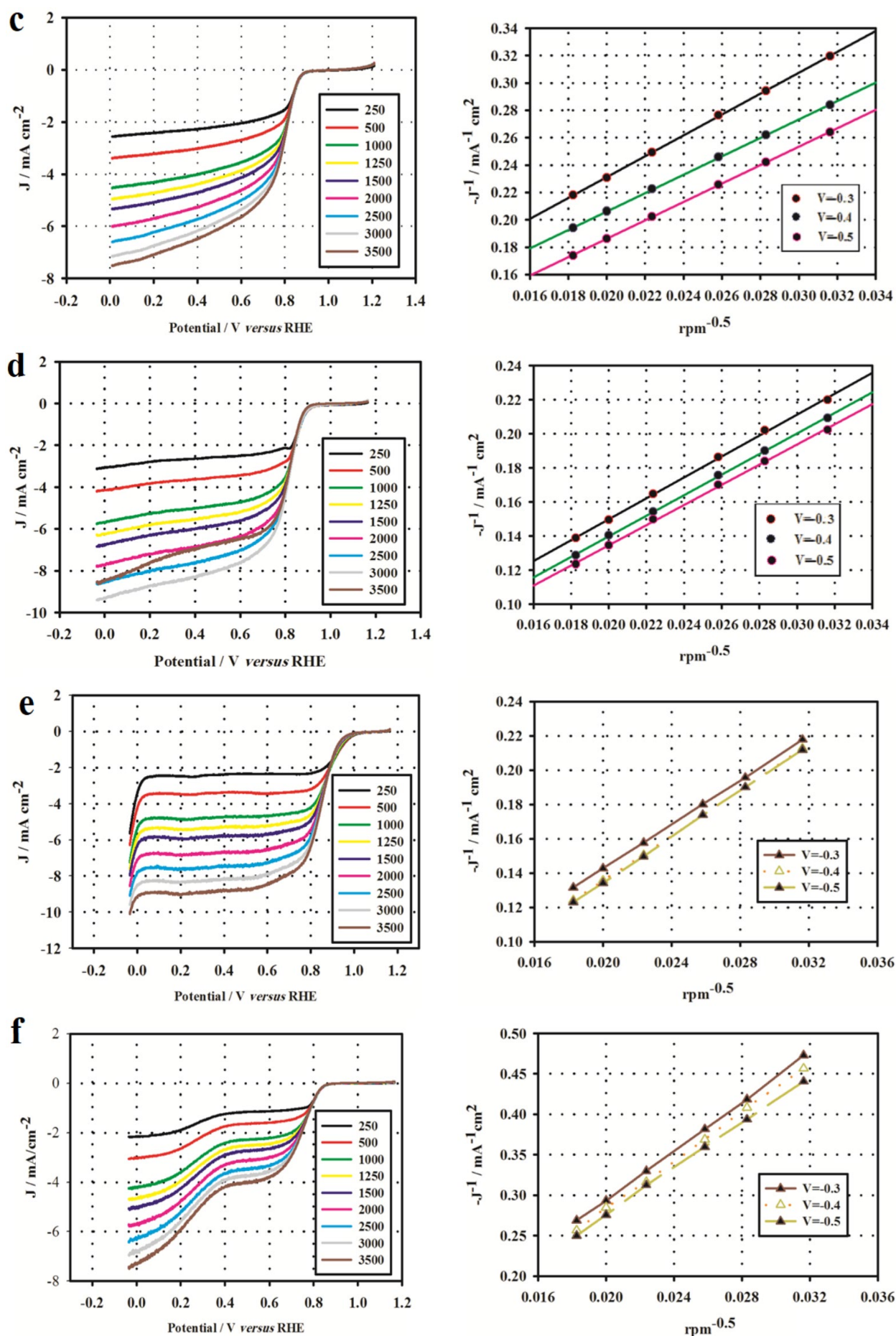
Figure 3. LSV at different rpm in KOH 0.1 M (scan rate 5 mV/s) and their Koutecky–Levich plots at different potentials for: GSP 900 (a), J300G-900 (b), S300G-900 (c), Gl300G-900 (d), Pt/C 20 wt % (e), and PG (f)

Table 1. The current density, onset potential, and electron transfer number of electrocatalysts

Electrocatalysts	Electron transfer Number (n)	Onset potential (V vs RHE)	Steady state current density (mA/cm²)
S300G-900	4.0	0.90	-5.4
Gl300G-900	4.0	0.93	-6.81
J300G-900	2.9	0.89	-3.52
GSP 900	4.1	0.93	-6.39
PG	2.2	0.85	-2. 70
Pt/C 20 wt %	4.0	0.99	-5.88
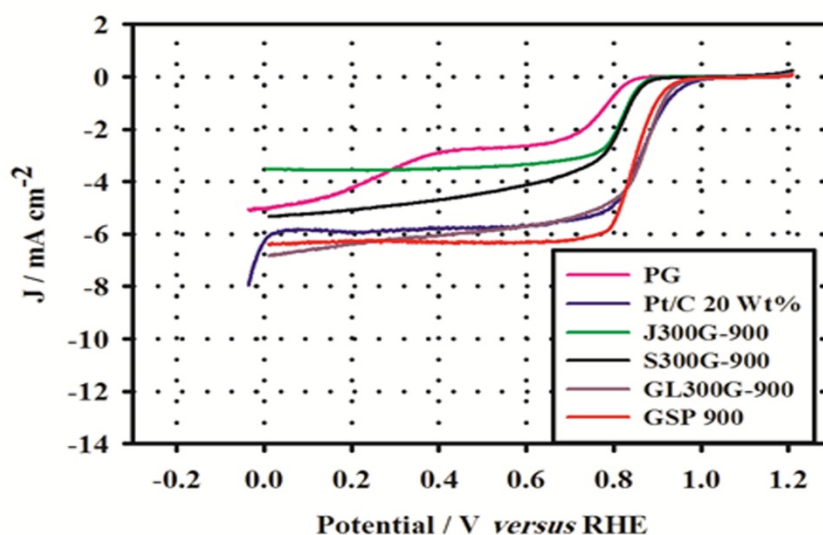
Figure 4. The LSV of electrocatalysts at 1500 rpm in O_2 saturated 0.1 M KOH

The PG electrode exhibited an ORR onset potential of almost 0.85 V (RHE). However, the onset potential of Gl300G-900, S300G-900 and J300G-900 electrodes was approximately 0.93, 0.93, and 0.89 V, which are more positive than PG. It can be suggested that due to the probability of heteroatom doping, the active sites of the synthesized electrocatalysts are enhanced and ORR is conducted in 4 electron pathways. The current density, onset potential, and electron transfer numbers of the synthesized electrocatalysts and Pt/C 20 wt % are compared in Table 1.

The electron transfer number of Gl300G-900, S300G-900, J300G-900, and GSP 900 samples in the ORR process was 4, 4, 2.9, and 4.1, respectively. The onset potential of Gl300G-900 and GSP 900 electrocatalysts is close to the Pt/C 20 wt %, and oxygen reduction is conducted via 4e⁻ pathway, too. The improved ORR electrocatalytic performance of heteroatom-doped samples can be explained by charge polarization according to quantum mechanics calculations. The changes in bond length, electronegativity, and one more extra electron (in the nitrogen atom) make in the carbon atom surface asymmetrical and cause more defects for the structures, which act as the active sites for the ORR. It should be mentioned that through multiple doping and by introducing more heteroatoms in the carbon structure, it is quite important to locate heteroatoms in specific (unique) positions and form suitable bonds such as the B-C–N in the Gl300-G900 sample in addition to individual effects [11].

4.1.3. Stability in the methanol solution

Morover, the catalytic current of the synthesized electrocatalyst (Gl300G-900, S300G-900, J300G-900 and GSP 900), Pt/C 20 wt %, and PG before and after methanol (1 M) addition in the ORR test were investigated, as shown in Figure 5.

The results represented that after methanol addition, the ORR peaks of PG and Pt/C 20 wt % electrocatalysts are reduced and disappeared, respectively. However, the CV measurements showed the stable and relatively unchanged hydrogen reduction peaks of the prepared doped electocatalysts after several CV cycles upon methanol addition, which represents good tolerance against crossover effects and remarkable stability in the doped electrocatalysts.

4.2. Structural characterization

The Gl300G-900 and GSP 900 heteroatom-doped samples were selected for structural analysis due to their improved electrochemical properties. The heteroatom doping level and defects in the graphene frameworke could be recognized using Raman spectroscopy.

Graphene displays three main peaks in Raman spectrum: G band ($\sim$1580 cm^{-1}) related to sp^2 carbon atoms vibrations as well as D ($\sim$1350 cm^{-1}) and 2D ($\sim$2680 cm^{-1}) bands corresponded to disordered sp^2 carbon atoms and defects due to introduced heteroatoms into its structure [24, 25]. The diordering and defects of the graphene structure could be defined as higher value of I_D/I_G (ratio of D to G band intensities).

The I_D/I_G values of PG, Gl300G-900, and GSP 900 samples are shown in Table 2. The higher values of I_D/I_G for Gl300G-900 (1.17) and GSP 900 (1.17) than PG (0.96) imply high disordering or defects level in the structure of the doped samples, leading to greater oxygen adsorption [25-27].
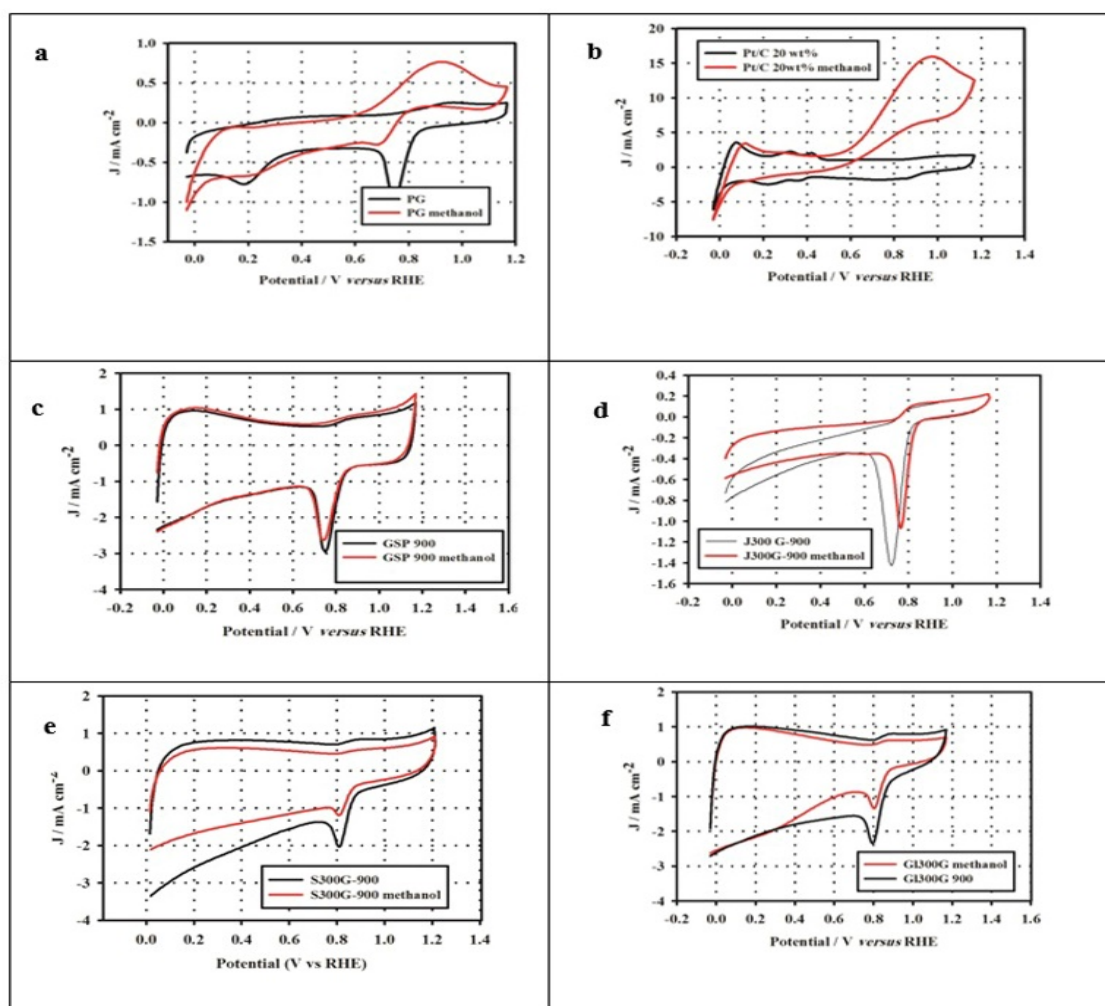
Figure 5. Cyclic voltammetry of (a) PG, (b) Pt/C 20 wt%, (c) GSP 900, (d) J300G-900, (e) S300-900, and (f) Gl300G-900 in KOH 0.1 M (scan rate: 50 mV/sec) by adding methanol

Table 2. Raman specification of the PG and heteroatom co-doped graphene

Sample	G band (cm^{-1})	D band (cm^{-1})	2D band (cm^{-1})	I_D/I_G
PG	1577.2	1341.85	2681.17	0.96
GSP 900	1577.12	1343.99	2679.13	1.17
Gl300G-900	1577.12	1343.99	2679.13	1.17

Fig. 6-a shows N_2 adsorption isotherms of PG and doped samples including Gl300G-900 and GSP 900. Typical type-IV isotherms with a loop beginning at the relative pressure approximately 0.4 were obtained, demonstrating that these materials have slit-shaped mesopores on the graphene structure [28]. Moreover, the average pore size distributions of the prepared electrocatalysts are given in Fig. 6-b. Also, the textural properties of the Gl300G-900 and GSP 900 electrocatalysts are shown in Table 3 and then, are compared to that of PG.

Moreover, the surface morphology and EDX image mapping analysis of the natural and chemical heteroatom doped samples (Gl300G-900 and GSP 900) were observed by FESEM (Fig. 7). The morphology of the prepared sample are similar to that of the graphene base. The elemental mapping distribution supports nitrogen, sulfur, boron, and phosphorous uniform dispersions in the pyrolyzed grape leaves sample, and the sample prepared using sulfur trioxide pyridine complex showed the presence of sulfur and nitrogen in the carbon structure.
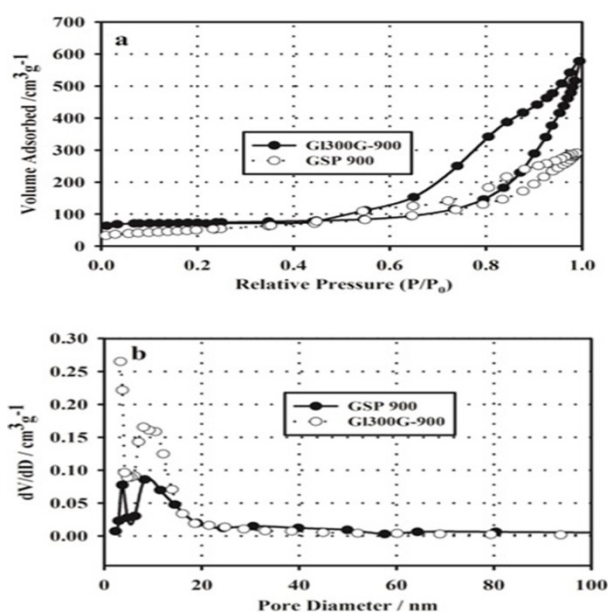

Figure 6. N_2 adsorption isotherms of PG and doped graphene (a), Pore size distribution of samples (b)

Table 3. Physical properties of PG and doped graphene

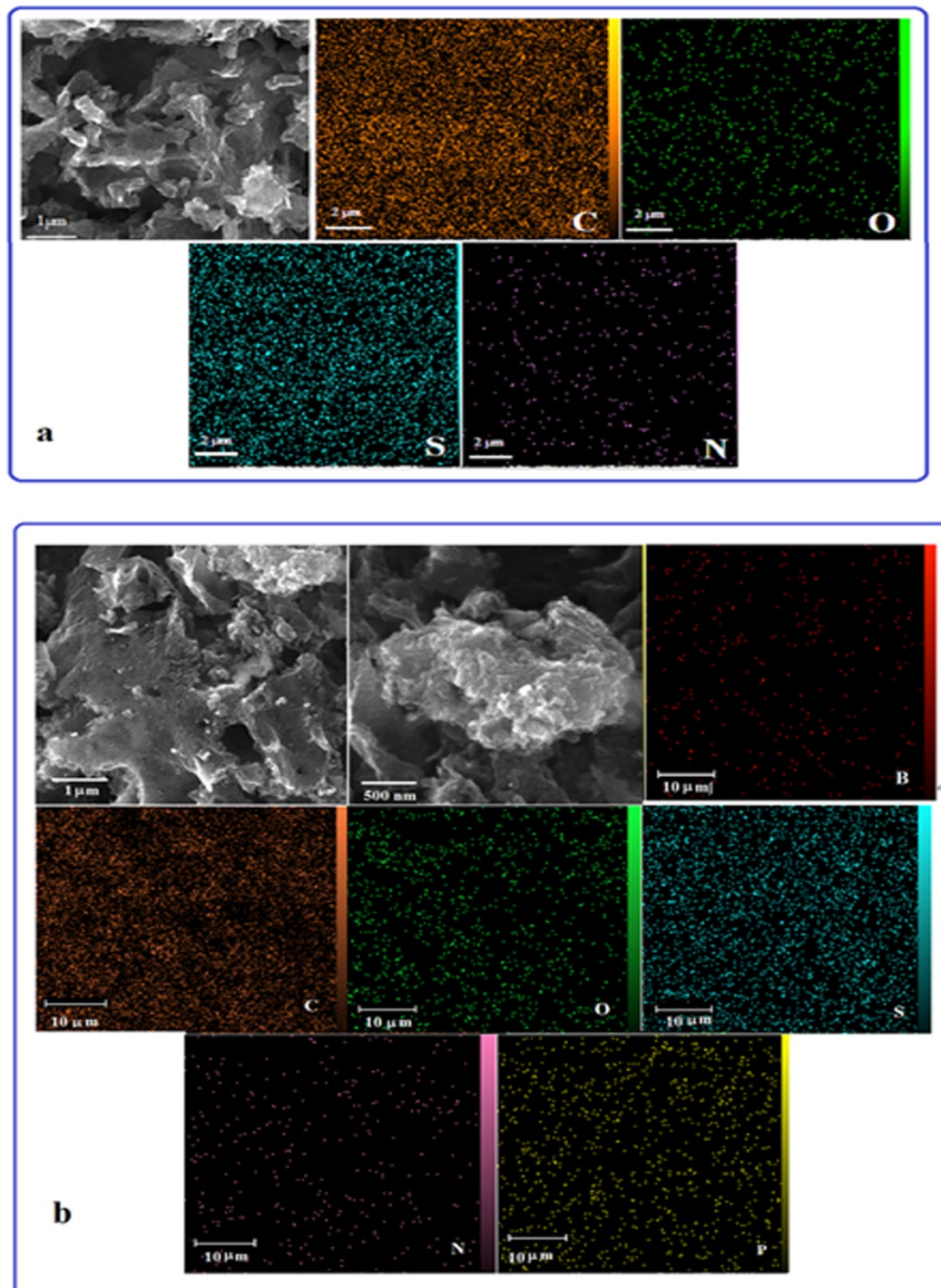| Electrocatalysts	BET surface area (m^2g^{-1})	Pore volume (cm^3g^{-1})	Mean pore size (nm)
PG	629.3	2.03	12.9
Gl300G-900	243.4	0.8	12.5
GSP 900	187.7`	0.44	9.7

Figure7. FESEM micrographs of prepared samples in two magnification and EDX mapping analysis of Carbon, Oxygen, sulfur, nitrogen, Boron, and Phosphorus in (a) the GSP 900, (b) the Gl300G-900 samples

In addition, the XPS analysis was applied to investigate the chemical bonding of the prepared samples, Gl300G-900 and GSP 900. Figure 8 shows that all the samples were included with a predominant narrow graphitic C 1s peak at approximately 284.4 eV.

Also, the adsorbed oxygen was seen in the samples as an O 1s peak at ~530 eV due to the physical incorporation of O_2 in the graphene framework. Moreover, the Gl300G-900 sample represents N 1s, S 2p, P 2p, and B1s peaks at ~400 eV, ~165 eV, ~133 eV, and ~190 eV, respectively. However, the GSP 900 sample shows only N 1s and S 2p peaks at approximately ~400 eV and ~165 eV, respectively.
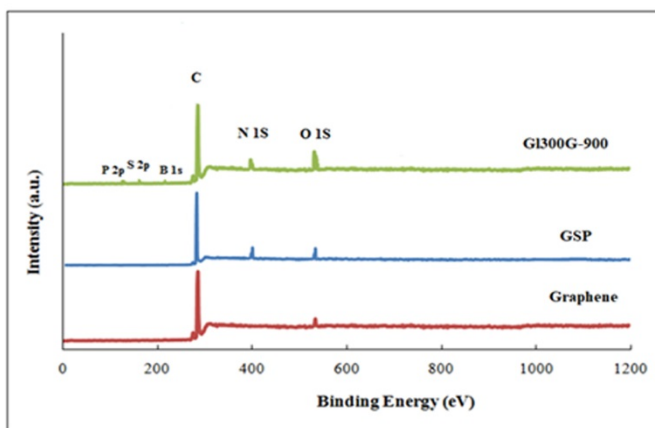
Figure 8. XPS survey for PG and as-synthesized samples

In addition, the high resolution XPS spectra for all the doped elements in GSP 900 and Gl300G900 samples are shown in Fig. 9 (a-b).

The pyridinic (~398.5 eV) and pyrrolic (~400.6 eV) species as the important phases with a nitrogen level of 2 % (at a ratio of 60 and 35 %, respectively) can be deconvluted from the high resolution N 1s XPS spectra in GSP 900 sample. Moreover, 5 % of the total N is present as oxidized forms (~403.2 eV) [1, 24, 29].

This result is important because pyridinic and graphitic species are suggested as the main ORR active sites due to allocation of one extra electron to the aromatic ring [29].

Also, three different peaks at approximately 163.8 (85 %), 165.0 (10 %), and 168.8 (5 %) were observed in the high-resolution S 2p spectra, which are related to $C-S_n-C$, $C=S$, sulfoxide specieses in the graphene framework [29-31]. In the high resolution spectrum of Gl300G-900, a strong S 2p peak (Fig. 9-b) shows a significant number of S doped atoms. Besides, the deconvolution analysis represents similar peaks of GSP 900 sample; however, at different intensities, around 46 % of sulfur in the Gl300G-900 sample appears in the sulfoxide forms in the graphene framework [29].
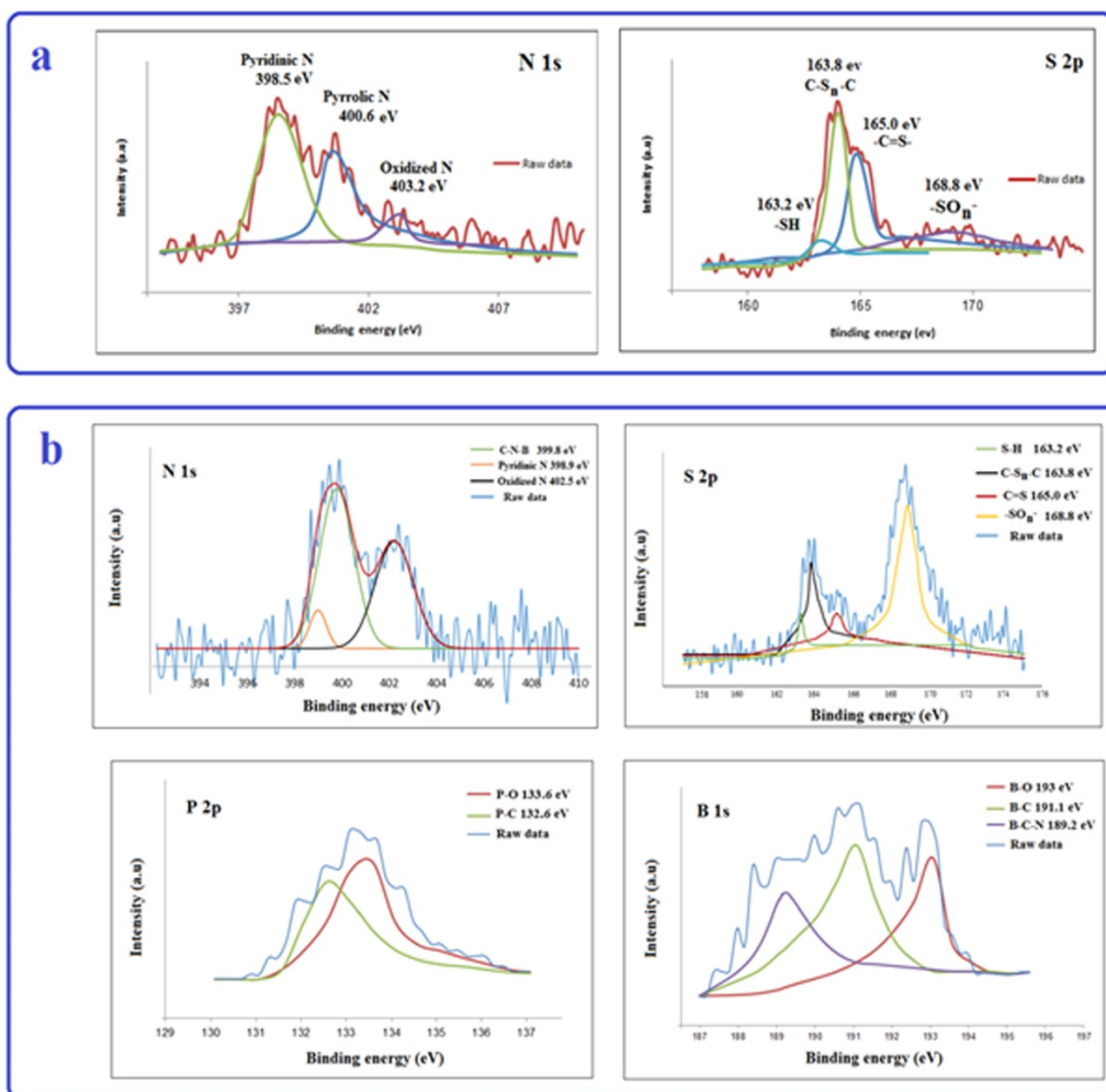
Figure 9. The HR-XPS spectra of prepared doped sample a:GSP 900, b:Gl300G-900

The HR-XPS of N 1s spectra of the Gl300G-900 sample can be resolved into three main peaks (Figure 9-b), related to pyridinic N (398.9 eV), nitrogrn in the N–B–C configuration (399.8 eV), and pyridinic N-oxide (402.5 eV) species [32-35].

The high resolution of B1s at approximately 193 eV (Fig. 9-b) is attributed to boron oxide. Also, the peak of 191 eV represents successful incorporation of boron atoms into the graphene framework. In this regard, the deconvolution

analysis of B1s shows three sub-peaks: B-C-N (189.2 eV), B-C (191.1 eV), and B-O (193 eV) bonds [32]. The XPS results confirm that N and B are covalently bound to the carbon in graphene structure, and N and B are covalently bound to each other (B–N bond) according to the peak of approximately 189.2 eV.

Moreover, deconvolution analysis of P 2p of Gl300G-900 (Fig. 9-b) represents the P-O and P-C binding energy peaks at approximately 133.6 eV and 132.6 eV, respectively, showing the P-doping feature [10]. The XPS results of element concentration, peaks position, and chemical state in the Gl300G-900 and GSP 900 samples are shown in Table 4.

Table 4. The XPS results of element concentration, peaks position, and chemical states in Gl300G-900 and GSP samples

Electrocatalyst	Element	%	Binding energy (eV)	Chemical state (%)
Gl300G-900	C	88.8		
	N	2.0	398.2	~10 %
			399.8	~50 %
			402.5	~40 %
	S	1.5	163.2	~7 %
			163.67	~34 %
			165.00	~13 %
			168.53	~46 %
	B	1.2	191.1	~42
			193	~30
			189.2	~28
	P	0.7	133.6	~64
			132.6	~36
	O	5.8		
GSP 900	C	93.1	284.4	
	N	2.0	398.5	~60 %
			400.6	~35 %
			403.2	~5 %
	O	4.0		
	S	0.9	163.8	~85 %
			165.0	~10 %
			168.8	~5 %

The XPS results indicate that sulfur, nitrogen, phosphorus, and boron are incorporated into the graphene framework. Therefore, heteroatoms have been successfully quaternary doped in the graphene framework and bound to carbon using high-temperature pyrolysis method [36].

4.3. Evaluation using microbial fuel cell

Furthermore, the optimal natural and chemical synthesized electrocatalysts (Gl300G-900 and GSP 900) were evaluated in the Microbial Fuel cell. In this regard, by changing external resistance from OCP to 4700, 3900, 3300, 2700, 2200, 1500, 1000, 910, 680, 510, 390 Ω, the polarization curves were obtained and the related voltages were recorded.

Figure 10 shows power density and steady state polarization curves for the Gl300G-900 and GSP 900 electrocatalysts in the MFC and the results are compared with the Pt /C 20 wt % and bare PG and electrocatalysts. The obtained results showed that the OCPs of the fuel cell with Gl300G-900, GSP 900, PG, and Pt/C 20 wt % electrocatalysts were 522 mV, 545 mV, 515 mV, and 647 mV, respectively. The Gl300G-900 and GSP 900 as the optimal synthesized cathodes in the MFC test showed high power density peaks of 31.5 mW m^{-2} and 30.9 mW m^{-2}, respectively, with much higher power density than the PG (18.0 mV m^{-2}) and close to the Pt/C 20 wt % (38.6 mW m^{-2}) cathodes, confirming the improved efficiency of these electrodes.

The increased power density of the prepared electrocatalysts using grape leaves as a natural source (Gl300G-900) compared to the PG could be explained because of

simultaneous doping of S, N, P, and B into the carbon framework and their synergetic effects. Also, the improved power density of the prepared sample using chemical source (GSP) compared to the PG was acheived due to the doping of S and N into the graphene framework.

Therefore, it is proposed that co heteroatom doping to the graphene structure leads to increase in the number of active sites and the electrocatalysts with improved performance as cathod catalysts could be obtained using natural and chemical sources.
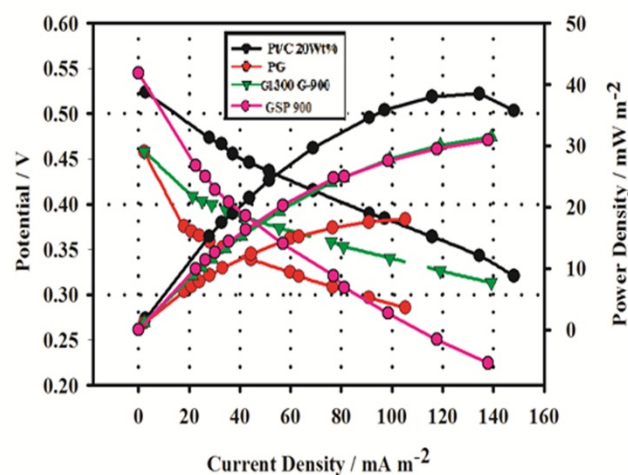

Figure 10. Power density and polarization and curves of MFC of the Gl300G-900 and GSP 900 samples at 25 ºC compared to the Pt/C 20 wt % and PG

5. CONCLUSIONS

This paper represents the preparation and characterization of heteroatoms-codoped porous graphene using garlic, grape leaves, microalgae Synechococcus elangatus, and sulfur trioxide pyridine complex. The optimal prepared electrocatalysts (Gl300G-900 and GSP 900) showed tolerance against methanol addition and long-term stability compared to the Pt/C 20 wt % and PG, with the onset potential and electron transfer number (0.93 vs RHE and 4.0) and (0.93 vs RHE and 4.1), respectively.

The electrochemical performance of the heteroatoms co-doped graphene (i.e., Gl300G-900 and GSP 900) represented high homogeneity of heteroatoms dispersion in the graphene framework, as well as a comparatively ORR performance versus Pt/C 20 wt %. The onset potential rates of the optimized electrocatalysts prepared using grape leaves (biomass resource) and sulfur trioxide pyridine complex (chemical source) were approximately 0.93 V vs RHE, being almost equal to Pt/C 20 wt % (0.99 V vs RHE). Furthermore, these electrocatalysts with excellent resistance towards methanol crossover effects conducted alkaline ORR in 4e$^-$ electron transfer pathway. Thus, the prepared electrocatalysts using grape leaves and sulfur trioxide pyridine complex are good candidates for ORR at low-temperature fuel cells instead of precious metal-based electrocatalysts due to its low cost and good performance. Moreover, grape leaves as an economic, safe, and environment-friendly precursor that include suitable heteroatoms with capability to introduce graphene structure seem to be valuable biomass materials for replacing Pt-based catalyst in large-scale commercialization.

6. ACKNOWLEDGEMENT

REFERENCES

1. Zhang, H., Wang, Y., Wang, D., Li, Y., Liu, X., Liu, P., Yang, H., An, T., Tang, Z. and Zhao, H., "Hydrothermal transformation of dried grass into graphitic carbon based high performance electrocatalyst for oxygen reduction reaction", *Small*, Vol. 10, (2014), 3371-3378. (https://doi.org/10.1002/smll.201400781).

2. Li, Y., Zhou, W., Wang, H., Xie, L., Liang, Y., Wei, F., Pennycook, S.J. and Dai, H., "An oxygen reduction electrocatalyst based on carbon nanotube-graphene complexes", *Nature Nanotechnology*, Vol. 7, (2012), 394-400. (https://doi.org/10.1038/nnano.2012.72).

3. Sui, S., Wang, X., Zhou, X., Su ,Y., Riffat, S. and Liu, C.J., "A comprehensive review of Pt electrocatalysts for the oxygen reduction reaction: Nanostructure, activity, mechanism and carbon support in PEM fuel cells", *Journal of Material Chemistry A*, Vol. 5, (2017), 1808-1825. (https://doi.org/10.1039/C6TA08580F).

4. Gupta, C., Maheshwari, P.H. and Dhakate, S.R., "Development of multiwalled carbon nanotubes platinum nanocomposite as efficient PEM fuel cell catalyst", *Materials for Renewable and Sustainable Energy*, Vol. 5, (2016), 1-11. (https://doi.org/10.1007/s40243-015-0066-5).

5. Workman, M.J., Dzara, M., Ngo, C., Pylypenko, S., Serov, A., McKinney, S., Gordon, J., Atanassov, P. and Artyushkov, K., "Platinum group metal-free electrocatalysts: Effects of synthesis on structure and performance in proton-exchange membrane fuel cell cathodes", *Journal of Power Sources*, Vol. 384, (2017), 30-39. (https://doi.org/10.1016/j.jpowsour.2017.02.067).

6. Venkateswara Rao, C., Cabrera, C.R. and Ishikawa, Y., "In search of the active site in nitrogen-doped carbon nanotube electrodes for the oxygen reduction reaction", *Journal of Physical Chemistry Letters*, Vol. 1, (2010), 2622-2627. (https://doi.org/10.1021/jz100971v).

7. Cheon, J.Y., Ahn, C., You, D.J., Pak, C., Hur, S.H., Kim, J. and Joo, S.H., "Ordered mesoporous carbon–carbon nanotube nanocomposites as highly conductive and durable cathode catalyst supports for polymer

electrolyte fuel cells", *Journal of Material Chemistry A*, Vol. 1, No. 4, (2012), 1270-1283. (https://doi.org/10.1039/C2TA00076H).

8. Jafri, R.I., Rajalakshmi, N. and Ramaprabhu, S., "Nitrogen-doped multi-walled carbon nanocoils as catalyst support for oxygen reduction reaction in proton exchange membrane fuel cell", *Journal of Power Sources*, Vol. 195, (2010), 8080-8083. (https://doi.org/10.1016/j.jpowsour.2010.06.109).

9. Zhang, H., Chen, J., Li, Y., Liu, P., Wang, Y., An, T. and Zhao, H., "Nitrogen-doped carbon nanodots@nanospheres as an efficient electrocatalyst for oxygen reduction reaction", *Electrochimica Acta*, Vol. 65, (2015), 7-13. (https://doi.org/10.1016/j.electacta.2015.02.240).

10. Qiao, X., Liao, S., You, C. and Chen, R., "Phosphorus and nitrogen dual doped and simultaneously reduced graphene oxide with high surface area as efficient metal-free electrocatalyst for oxygen reduction", *Catalysts*, Vol. 5, (2015), 981-991. (https://doi.org/10.3390/catal5020981).

11. Sadegh Hassani, S. and Samiee, L., Carbon nanostructured catalysts as high efficient materials for low temperature fuel cells, Hanbook of ecomaterials, Springer International Publishing, (2018). (https://doi.org/10.1007/978-3-319-48281-1_79-1)..

12. Arjmandi-Tash, H., Belyaeva, L.A. and Schneider, G.F., "Single molecule detection with graphene and other two-dimensional materials: nanopores and beyond", *Chemical Society Reviews*, Vol. 45, (2015), 476-493. (https://doi.org/10.1039/C5CS00512D).

13. Palaniselvam, T., Valappil, M.O., Illathvalappil, R. and Kurungot, S., "Nanoporous graphene by quantum dots removal from graphene and its conversion to a potential oxygen reduction electrocatalyst via nitrogen doping", *Energy & Environmental Sciences*, Vol. 7, No. 3, (2014), 1059-1067. (https://doi.org/10.1039/c3ee43648a).

14. Rivera, L.M., Fajardo, S., Arévalo, M.D.C., García, G. and Pastor, E., "S and N-doped graphene nanomaterials for the oxygen reduction reaction", *Catalysts*, Vol. 7, No. 9, (2017), 278-290. (https://doi.org/10.3390/catal7090278).

15. Wang, X., Sun, G., Routh, P., Kim, D.H., Huang, W. and Chen, P., "Heteroatom-doped graphene materials: Syntheses, properties and applications", *Chemical Society Reviews*, Vol. 43, (2014), 7067-7098. (https://doi.org/10.1039/C4CS00141A).

16. Daems, N., Sheng, X., Vankelecom Ivo, F.J. and Pescarmona, P.P., "Metal-free doped carbon materials as electrocatalysts for the oxygen reduction reaction", *Journal of Material Chemistry A*, Vol. 2, (2014), 4085-4110. (https://doi.org/10.1039/C3TA14043A).

17. Guo, C., Liao, W., Li, Z., Sun, L. and Chen, C., "Easy conversion of protein-rich enoki mushroom biomass to nitrogen-doped carbon nanomaterial as a promising metal-free catalyst for oxygen reduction reaction", *Nanoscale*, Vol. 7, No. 38, (2015), 15990-15998. (https://doi.org/10.1039/C5NR03828F).

18. Guo, C., Sun, L., Liao, W. and Li, Z., "The use of an edible mushroom-derived renewable carbon material as a highly stable electrocatalyst towards four-electron oxygen reduction", *Materials*, Vol. 9, No. 1, (2016), 1-11. (https://doi: 10.3390/ma9010001).

19. Sadegh Hassani, S., Ziaedini, A., Samiee, L., Dehghani, M., Mashyekhi, M. and Faramarzi, M.A., "One step synthesis of tertiary co-doped graphene electrocatalyst using microalgae synechococcus elangatus for applying in microbial fuel cell", *Fuel Cells*, Vol. 19, No. 5, (2019), 623-634. (https://doi.org/10.1002/fuce.201800167).

20. Sadegh Hassani, S., Ganjali, M.R., Samiee, L., Rashidi, A.M., Tasharrofi, S., Yadegari, A., Shoghi, F. and Martel, R., "Comparative study of various types of metal free N and S co-doped porous graphene for high performance oxygen reduction reaction in alkaline solution", *Journal of Nanoscience and Nanotechnology*, Vol. 18, (2018), 4565-4579. (https://doi.org/10.1166/jnn.2018.15316).

21. Pourmand, S., Abdouss, M. and Rashidi, A.M., "Preparation of via nanoporous zinc oxide and its application as a nano adsorbent for benzene, toluene and xylenes removal", *International Journal of Environmental Research*, Vol. 9, (2015), 1269-1276. (https://doi.org/10.22059/IJER.2015.1018).

22. Qu, L.T., Liu, Y., Baek, J.B. and Dai, L.M., "Nitrogen-doped graphene as efficient metal-free electrocatalyst for oxygen reduction in fuel cells", *ACS Nano*, Vol. 4, (2010), 1321-1326. (https://doi.org/10.1021/nn901850u).

23. Lin, Z., Waller, G., Liu, Y. and Wong, C.P., "3D nitrogen-doped graphene prepared by pyrolysis of graphene oxide with polypyrrole for electrocatalysis of oxygen reduction reaction", *Nano Energy*, Vol. 2. (2013), 241-248. (https://doi.org/10.1016/j.nanoen.2012.09.002).

24. Xing, Z., Ju, Z., Zhao, Y., Wan, J., Zhu, Y., Qiang, Y. and Qian, Y., "One-pot hydrothermal synthesis of nitrogen-doped graphene as high-performance anode materials for lithium ion batteries", *Scientific Reports*, Vol. 6, (2016), 26146-26158. (https://doi.org/10.1038/srep26146).

25. Ai, W., Luo, Z., Jiang, J., Zhu, J., Du, Z., Fan, Z., Xie, L., Zhang, H., Huang, W. and Yu, T., "Nitrogen and sulfur codoped graphene: multifunctional electrode materials for high performance Li ion batteries and oxygen reduction reaction", *Advanced Materials*, Vol. 26, (2014), 6186-6192. (https://doi.org/10.1002/adma.201401427).

26. Sun, Z., Masa, J., Weide, P., Fairclough, S.M., Robertson, A.W., Ebbinghaus, P., Warner, F.H., Tsang, S.C.E., Muhlerb, M. and Schuhmann, W., "High-quality functionalized few-layer graphene: facile fabrication and doping with nitrogen as a metal-free catalyst for the oxygen reduction reaction", *Journal of Material Chemistry A*, Vol. 3, (2015), 15444-15450. (https://doi.org/10.1039/C5TA02248G).

27. Brunauer, S., Deming, L.S., Deming ,W.E. and Teller, E., "On a theory of the van der Waals adsorption of gases", *Journal of the American Chemical Society*, Vol. 62, No. 7, (1940), 1723-1732. (https://doi.org/10.1021/ja01864a025).

28. Ma, C.B., Zhu, Z.T., Wang, H.X., Huang, X., Zhang, X., Qi, X., Zhang, H.L., Zhu, Y., Deng, X., Peng, Y., Hand, Y., Zhang, H. and Lu, L., "Covalent entrapment of cobalt–iron sulfides in N-doped mesoporous carbon: Extraordinary bifunctional electrocatalysts for oxygen reduction and evolution reactions", *ACS Applied Materials & Interfaces*, Vol. 7, (2015), 1207-1218. (https://doi.org/10.1021/am507033x).

29. Wu, Z.S., Yang, S., Sun, Y., Parvez, K., Feng, X. and Mullen, K., "3D nitrogen-doped graphene aerogel-supported Fe_3O_4 nanoparticles as efficient electrocatalysts for the oxygen reduction reaction", *Journal of the American Chemical Society*, Vol. 134, (2012), 9082-9085. (https://doi.org/10.1021/ja3030565).

30. Bag, S., Mondal, B., Das, A.K. and Raj, C.R., "Nitrogen and sulfur dual-doped reduced graphene oxide: Synergistic effect of dopants towards oxygen reduction reaction", *Electrochimica Acta*, Vol. 163, (2015), 16-23. (https://doi.org/10.1016/j.electacta.2015.02.130).

31. Su, Y., Zhang, Y., Zhuang, X., Li, S., Wu, D., Zhang, F. and Feng, X., "Low-temperature synthesis of nitrogen/sulfur co-doped three-dimensional graphene frameworks as efficient metal-free electrocatalyst for oxygen reduction reaction", *Carbon*, Vol. 62, (2013), 296-301. (https://doi.org/10.1016/j.carbon.2013.05.067).

32. Dou, S., Huang, X., Ma, Z., Wu, J. and Wang, S., "A simple approach to the synthesis of BCN graphene with high capacitance", *Nanotechnology*, Vol. 26, (2015), 045402. (https://doi.org/10.1088/0957-4484/26/4/045402).

33. Chen, X., Chen, X., Xu, X., Yang, Z., Liu, Z., Zhang, L., Xu, X., Chen, Y. and Huang, S., "Sulfur doped porous reduced graphene oxide hollow nanosphere frameworks as metal free electrocatalysts for oxygen reduction reaction and as supercapacitor electrode materials", *Nanoscale*, Vol. 6, No. 22, (2014), 13740-13747. (https://doi.org/10.1039/C4NR04783D).

34. Dong, Y., Pang, H., Yang, H.B., Guo, C., Shao, J., Chi, Y., Li, C.M. and Yu, T., "Carbon based dots co-doped with nitrogen and sulfur for high quantum yield and excitation independent emission", *Angewandte Chemie International Edition*, Vol. 52, (2013), 7800-7804. (https://doi.org/10.1002/anie.201301114).

35. Wang, Y., Zhang, B., Xu, M. and He, X., "Tunable ternary (P,S,N) – doped graphene as an efficient electrocatalyst for oxygen reduction reaction in an alkaline medium", *RSC Advances*, Vol. 5, No. 105, (2015), 86746-86753. (https://doi.org/10.1039/C5RA18251D).

36. Lin, H., Chu, L., Wang, X., Yao, Z., Liu, F., Ai, Y., Zhuang, X. and Han, S., "Boron, nitrogen and phosphorous ternary doped graphene aerogel with hierarchically porous structures as highly efficient electrocatalysts for oxygen reduction reaction", *New Journal of Chemistry*, Vol. 40, (2016), 6022-6029. (https://doi.org/10.1039/C5NJ03390J).